Analysis of Slope Failure Mechanism at the East Pit of Daye Iron Ore Mine

J. Li
B.E., M.Sc.
Ph.D. Student, Western Australian School of Mines, Australia
E. Villaescusa
B.E.(Hons), M.Sc., Ph.D.
Professor of Mining Geomechanics, Western Australian School of Mines, Australia

Summary The East Pit of Daye iron ore mine is the deepest iron ore open pit in China. Several slope failures have occurred since the 1970s, and over the years engineering geological and hydrogeological investigations in conjunction with surface displacement monitoring have been carried out. This paper discusses the mechanism of the slope failure and the factors inducing a major landslide of approximately 9000 m^3 in volume which was experienced over the hangingwall of a major fault where large deformations were recorded. The results of engineering geology investigations, hydrogeology studies and surface deformation monitoring are presented.

1. INTRODUCTION

The Daye iron ore mine is located at Tieshan District, Huangshi, Hubei, China, The mine is the biggest iron ore supplier for Wuhan Iron and Steel Corporation, Pty Ltd. The East Pit is the main iron ore producer among Daye's four open pits and underground stopes. Its annual production is up to 40 percent of the overall production of Daye. Other products in the iron ore concentrate are copper, sulphur, cobalt and gold.

The mine design sector A in which the landslides occurred is located to the west of the hangingwall of the ore body. It represents the northwest wall of the East Pit slope. On April 30, 1990, a landslide (A_1) through the hangingwall of the fault F_9 occurred. Approximately 6000m^3 of material slid from 0 mRL to 72 mRL. Reinforcement was installed prior to the failure in the form of 15 to 20m long rock bolts in conjunction with mesh and shotcrete. The reinforcement scheme was designed to minimise the deformations of the hangingwall slope of the fault F_9. The reinforcement scheme did not perform well and a triangular area of rock mass in the hangingwall of the fault F_9 continued to deform between 48 mRL to 180 mRL. The excessive movement which caused the initial slide A_1, was the precursor to the massive slide (9000 m^3 in volume), experienced in July 1996. This slide was successfully predicted and no casualty or damage to equipment occurred (Ge, *et al*, 1997).

In this study the causes and failure mechanism of the larger slide are analysed. Results of engineering geology investigations, hydrogeology studies and surface deformation monitoring are used in the analysis.

2. GEOLOGICAL BACKGROUND

2.1 Engineering Geology

The primary rock type of sector A is a hard biotite diopside diorite ($BD\delta^2$) which constitutes the primary lithology and covers three quarters of the slope. Other rock types are albitite and orthoclase altered diorite ($BD\delta^2_{AO}$), kaolinite and chlorite altered diorite ($BD\delta^2_{KC}$) as well as quartz-bearing kaolinite and chlorite-altered diorite ($BD\delta^1_{KC}$). The kaolinite and chlorite altered rock masses are very weak.

The slope stability of this area is controlled by northwest and north northeast trending structures. Fault F_9 is representative of northwest trending structures and cuts the slope at an oblique angle. The fault can be divided into three sections. The first section is defined from 72 mRL and up to the crest of slope with an orientation of 68°/200°. It is 2 ~ 5m wide and highly altered with chlorite, kaolinite, montmorillonite and illite minerals. The fault bifurcates at the 72 mRL and forms sections two and three. The fault on the second section (F_9') is orientated approximately 60°/180° and disappeared after becoming a smooth plane between 48 mRL to 0 mRL. The third section comprises the lowest part of the fault F_9 extended -84 mRL with an orientation of 60°/220°. The width of the last section of the fault ranges from 3 to 5m. Below 48 mRL, the north-east striking discontinuities intersect the fault F_9 several times and move it south-south west as shown on Figure 1.

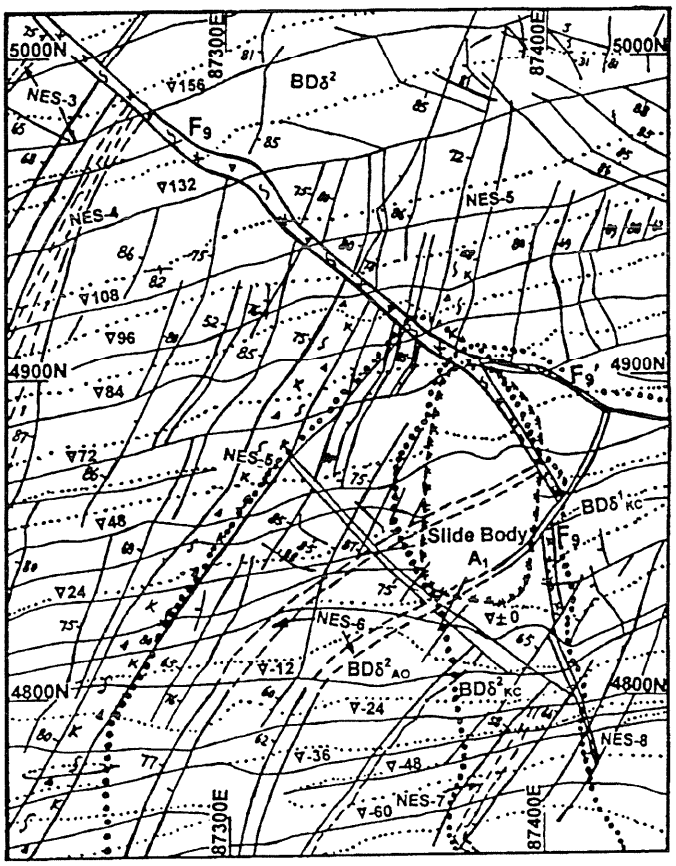

Figure 1. Engineering geology plan of sector A.

Several north northeast striking discontinuities, including small faults were present on this pit sector. These discontinuities appeared to control the failure geometry. Figure 2 is a lower hemisphere equal area projection showing pole contours of the north-east striking family of discontinuities. These features are shown with respect to the orientations of the slope sector and the first section of the fault F_9. Almost 90% of the faults have a northeast strike, with an average orientation of 75°/298°.

2.2 Hydrology

The Daye mine is located in an area that holds a temperate and moist climate, with abundant rainfall. Most rainfall is experienced between April and August. The average precipitation is 1386 mm, with a maximum of 2212 mm and 249 mm per year and day respectively. Average precipitation conditions were experienced from 1990 to 1995, the period of this study.

The permeability of the diorite rock mass is very low, with less than 0.001m per day recorded. The permeability along the fault F_9 is also very low due to swelling clays such as chlorite, illite and montmorillonite which are present as fracture fillings.

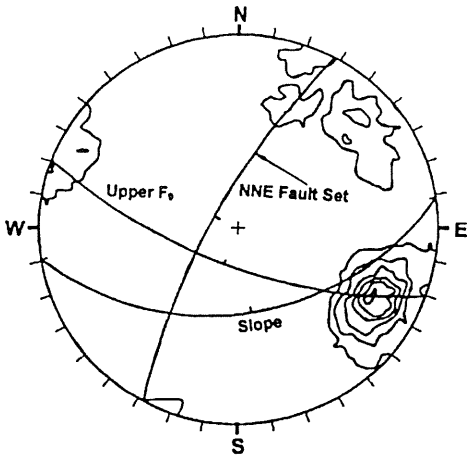

Figure 2. Stereographic projection of main faults and slope.

Two drainage ditches on benches 156 mRL and 96 mRL were constructed to block the slope surface runoff. These ditches were blocked up by loose material and damaged due to the slope deformation resulting in a great deal of water flowing down and

seeping into the lower slope. The rainfall is the main water supply source for the hangingwall rock mass of the fault F_9, as there is not any other water bodies, such as a reservoir around the east pit, except for a small early waste dump on top of the north wall (above 265 mRL).

3. HANGINGWALL ROCK MASS DEFORMATION OF FAULT F_9

Following the initial slide A_1, the rock mass around the fault F_9 was cracked, and evidence of slope deformation was clearly apparent. This deformation could not be stopped despite the installation of 15 ~ 20m long reinforcement elements. Anchors were installed between 12 mRL to 84 mRL. Mesh and shotcrete were used to increase the holding capacity of the overall reinforcement scheme. A triangular area of deformation was experienced from 180 mRL to 48 mRL. This eventually led to a large failure, which resulted in 9000m^3 of slide material.

Figure 3 shows tensile cracks that were oriented to the north, northeast striking faults and fracture zones. Along the west boundary of instability, tensile cracks ❶, ❷, ❸ and ❹ on mesh and shotcrete surface were defined between 72 mRL to 108 mRL. When a crack opening between 10 to 40 cm in width was recorded a 15m of deformation was experienced towards the northwest. New tensile cracks (❺, ❻, ❼) were also formed at this stage. Crack ❽ that was near a surface displacement monitoring point 84-9 around 84 mRL was developed in 1993. This crack which crossed the fault F_9 from hangingwall to footwall had a measured width of 760 to 1000 mm in early 1995. However, the weathered and altered broken rock under the shotcrete in the footwall did not move all the time. Cracking in the shotcrete around the footwall slope surface was induced (pulled and squeezed) by the movement of the hangingwall rock masses.

Figure 4 shows horizontal displacement vectors of the hangingwall slope within 50m of the fault F_9, where displacements were measured with SETA 20 laser transit and the monitoring period was 3 days to one month depending upon the precipitation and displacement rate experienced. The vectors above 48 mRL are almost parallel to the strike of fault F_9. The maximum horizontal displacement of 2417.0 mm was recorded at monument 96-8 up to June 7, 1996. Figure 4 also shows that the slope below 24 mRL deformed with a maximum displacement of 550 mm recorded. Several measures were adopted to enhance the stability of the lower part of the slope, including a repair of the drainage ditches on 156 mRL and 96 mRL. Rail piles were installed on the bench berms. Subhorizontal bolts (15 to 20m long) in conjunction with mesh and shotcrete were also used.

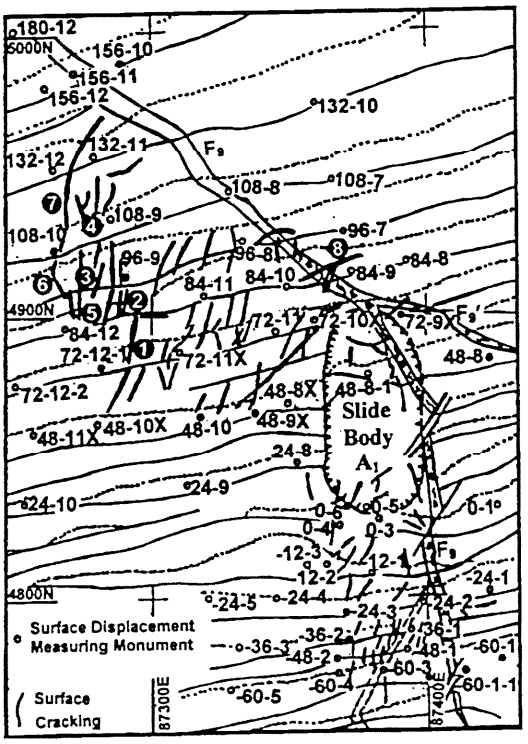

Figure 3. Tensile cracks measured on slope surface.

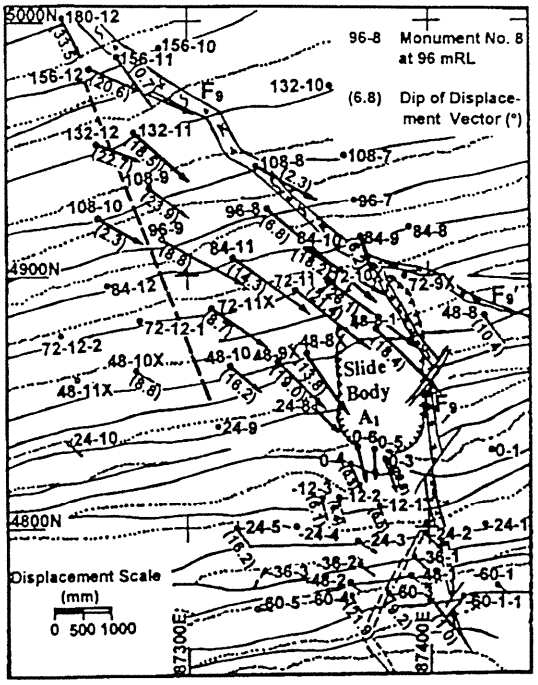

Figure 4. Slope surface displacement vectors.

4. FAILURE MECHANISM OF FAULT F_9 HANGINGWALL SLOPE

Three major types of toppling failure have been described for hard rock slopes (Hoek and Bray, 1981). The basic requirements to form a toppling failure are a subvertical discontinuity system, a parallel free face to the discontinuity system (the

discontinuities usually plunge into the free face), and mainly horizontal deformation caused by bending and flexure. According to the macroscopic investigation and displacement data analysis, the mechanism of deformation and failure of hangingwall along the fault F_9 was a flexural toppling, but with different characteristics in nature.

The north, north-east striking faults and squeezing zones separated the rock mass into a series of thin layers that were subvertically oriented and plunging towards the free face defined by the slide body A_1 and the slope face. The measured spacing of joints and faults was 0.1 to 0.4m with a maximum of 0.8m. The slope and free face caused by the slide body A_1 weakened the rock mass, which lost confinement. The fault F_9 represented the northeast boundary of the unstable zone. The overall failure was a complex combination of plane shear and toppling. The slope and fault orientations (43°/170° and 68°/200°, respectively) provided a geometrical condition for a landslide, while the north, northeast structures (oriented 75°/298°) provided the structural condition for toppling and sliding (see Figure 2).

Observation of the loading conditions on the slope indicated that the rock mass in the slope had been disturbed following the initial A_1 slide. Deformations with a subsequent stress redistribution were experienced all the way to 180 mRL as shown in Figure 3. Production from the pit continued with the slope deepening from 336m to 396m when the second slide occurred.

Analysis of the displacement vectors suggests that the largest horizontal movement was experienced near the fault F_9. Very small deformations were recorded in the west side of the unstable area. Overall, the failure geometry became gradually narrower, and the recorded displacements decreased from 48 mRL to 180 mRL (see Figure 5). The slide is deeper close to the fault F_9 and becomes more and more shallow westwards. Thus, at a first glance, the shape of the failure initially looks like a wedge. However, an in depth investigation and analysis suggests that the mode of this failure is a toppling and plane shearing.

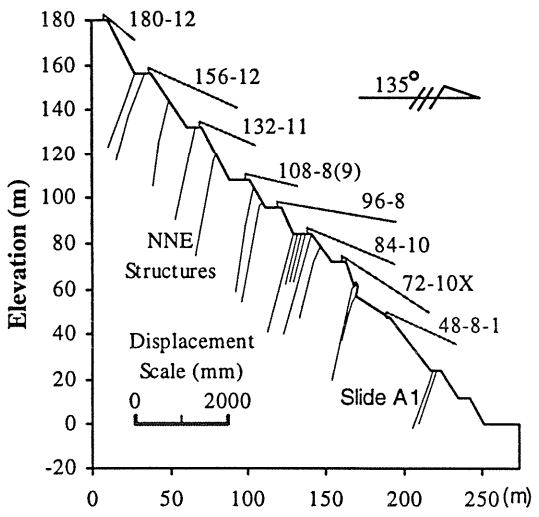

Figure 5. Slope toppling deformation section at sector A.

The external forces accelerating and promoting the displacement and finally leading to failure were slope ground water pressure. As mentioned before, diorite rock masses and the faults filled by kaolinite and montmorillonite are relatively impermeable. In the rainy season, water infiltrated into open joints, faults and tensile cracks, creating a build up of water pressure. The heavier the rainfall, the higher the water pressure in the tensile cracks and open fractures. Another effect of water was softening and strength reduction of the rock mass. Figure 6 and Table 1 shows displacements and their rates at different seasons on the six surface monitoring locations. The data suggests an increased rate of movement in the rainy season. Little changes were experienced during the dry seasons. The critical displacement rate monitored was 2.0 mm/d. The data showed that above this limit, a slope failure would be developed. An increased rate of displacement (up to 24.0 mm/d) that eventually led to failure was experienced in May and early June of 1996. Excessive rainfall had been experienced from March to July when the failure occurred. In March, it almost rained daily with a maximum precipitation of 197 mm/day. In June, the total rainfall was 609 mm. Finally, the failure occurred on July 2 when a 117 mm rainfall was experienced.

Table 1. Horizontal displacement rates of some monitoring points (mm/day).

Point No	4/93 ~ 9/93	10/93 ~ 3/94	4/94 ~ 7/94	8/94 ~ 3/95	4/95 ~ 8/95	9/95 ~ 1/96	2/96 ~ 4/96	5/96 ~ 6/96
96-8	0.66	0.46	1.75	0.15	1.03	0.48	2.83	23.95
72-11	0.55	0.30	1.30	0.09	0.83	0.28	2.36	14.92
48-8-1	0.65	0.27	1.43	0.07	0.90	0.34	2.58	16.63
0-3	0.38	0.25	0.45	0.0	0.38	0.10	1.06	4.82
-36-1	—	—	0.34	0.11	0.22	0.18	0.78	1.63
-60-2	—	—	0.42	0.01	0.18	0.14	0.78	1.00

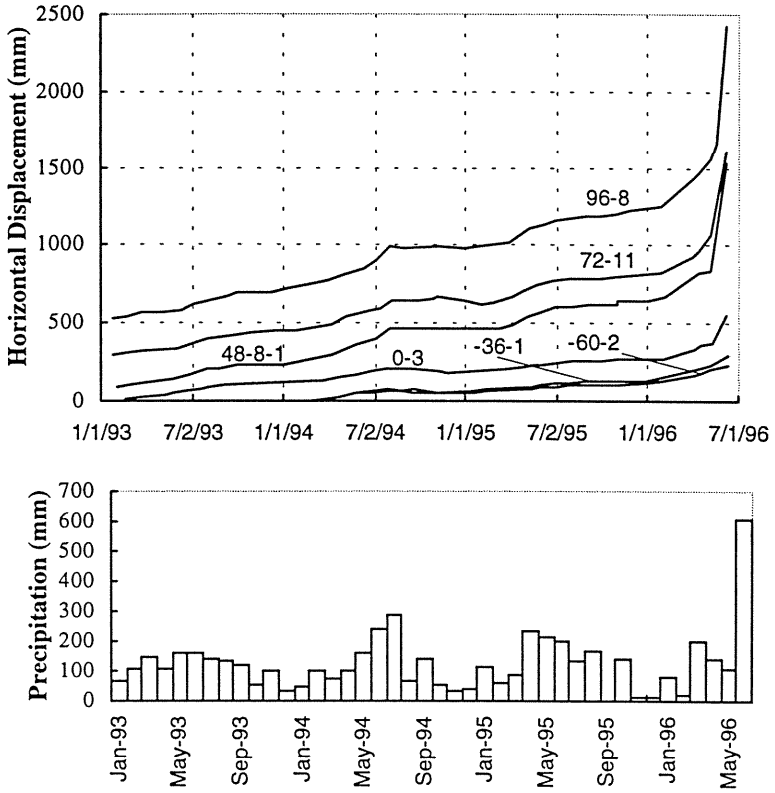

Figure 6. The relationships of horizontal displacement versus time and precipitation.

Analysis of Figure 6 and Table 1 indicates that the surface displacements were linked to rainfall and increased steadily from March to June. The slope was under a typical progressive failure condition as described by Savely (1993).

5. CONCLUSIONS

Since the initial landslide A_1 took place in early 1990, deformation observation and displacement monitoring have been conducted over the hangingwall slope of the fault F_9. Engineering geological as well as hydrogeological investigations had been carried out. According to the analysis, the failure was geologically controlled by the main fault F_9 and the north, northeast striking faults. The free faces were controlled by the early slide A_1 and also the slope face, the triggering factor was the rainfall, and the failure mechanism was very complex including a combination of toppling and plane shearing.

6. ACKNOWLEDGEMENTS

The authors wish to thank the Daye iron ore mine for the permission to publish this paper. The first author is grateful to Dr Chuanzhi Xiong, Professor of Chansha Research Institute of Mining and Metallurgy, Hunan, China. The second author acknowledges the financial support from the Australian Centre for Geomechanics and Curtin University of Technology for his position as professor of Mining Geomechanics at the Western Australian School of Mines. The Australian Centre for Geomechanics has received funding for this position from the Government of Western Australia, Centres of Excellence Program.

7. REFERENCES

Ge X., *et al* (1997). Study on prediction of landslide of rock slope, *The First Asian Rock Mechanics Symposium on Environmental and Safety Concerns in Underground Construction,* Lee, Yang, Chung (eds), Balkema, Rotterdam.

Hoek, E., Bray, J. (1981). *Rock Slope Engineering*, 3rd ed., E & FN SPON, London, 358p.

Savely, J. P. (1993). Slope management strategies for successful mining, *Proceedings of The International Congress on Mine Design*, Canada, Bawden & Archibald (eds),Balkema, Rotterdam.